

Supplementary Material

Details for the pulse sequence

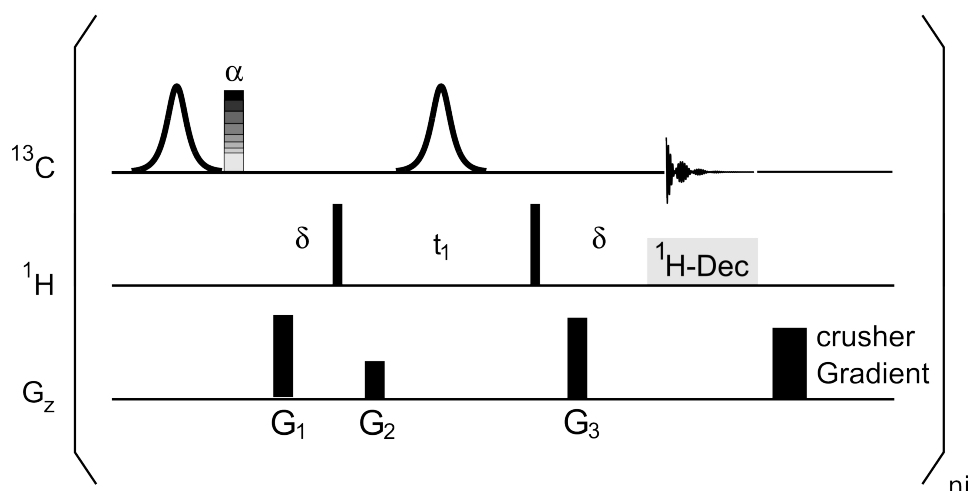


Figure S1. Pulse sequence for the fast acquisition of 2D-HMQC-NMR spectra. The adiabatic ^{13}C π pulses had a hypersecant shape with the pulse length set to 1ms to avoid losses arising from B1 field inhomogeneity. The small excitation flip angle on ^{13}C was successively increased (from 10° to 30°) to compensate for relaxation and the decrease of available magnetization for higher increments. Pulsed field selection gradients G_1 , G_2 and G_3 of 1ms were executed at -36, 14.4 and +36 G/cm. The dephasing of the first gradient (G_1) (^{13}C single quantum) is proportional to γ_C , the dephasing of the second gradient (G_2) to $\gamma_C + \gamma_H$ (^1H - ^{13}C double quantum) and the refocusing gradient (G_3) is proportional to γ_C , hence

$$G_1\gamma_C + G_2(\gamma_C + \gamma_H) = G_3\gamma_H$$

with arbitrarily chosen $G_1 = -G_3$

it follows that

$$G_2 = 2G_3 \gamma_C / (\gamma_C + \gamma_H)$$

Considering that $\gamma_H = 4\gamma_C$, it follows that $G_2 = 0.4G_3$. Therefore if $G_3 = 36$ then $G_2 = 14.4$. The crusher gradient was executed at 21 G/cm and was essential to minimize artifacts arising from remaining transverse magnetization after acquisition, probably arising from stimulated echoes in subsequent increments.

Variable flip angle excitation

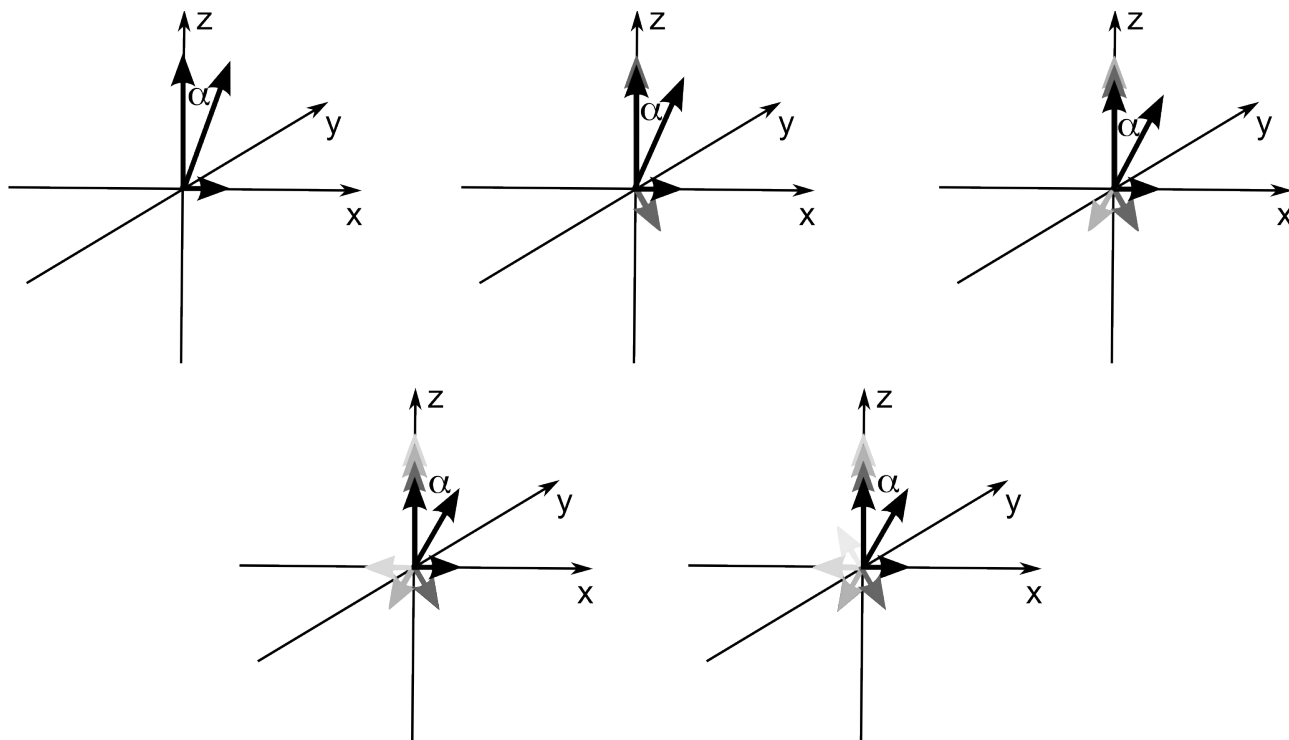


Figure S2. Schematic representation of magnetization evolving during the execution of the pulse sequence. The first image shows the situation after the first small flip angle excitation. Subsequently the transverse magnetization develops its chemical shift, then in the next increment new transverse magnetization is created from the remaining longitudinal magnetization. This is repeated throughout the 2D experiment. The flip angle is increased from increment to increment to prevent the transverse magnetization from decaying too fast.

Non-Uniform Sampling

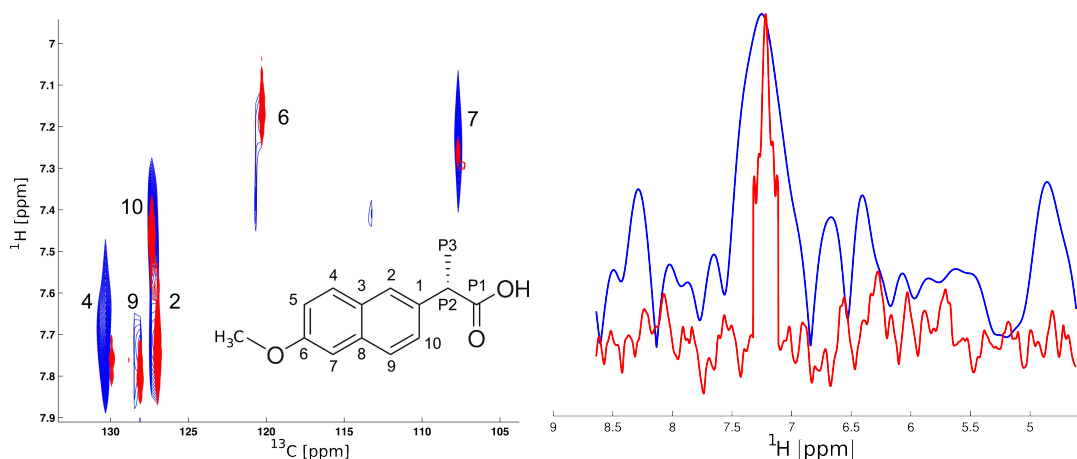


Figure S3. 2D-HMQC and 1D-slice for naproxen. To reduce the line width in the incremented dimension of the 2D spectrum a non-uniform sampling schedule was applied. The maximum evolution time $t_{1,max}$ was extended to the 4-fold value compared to conventional sampling. Sampling points were chosen randomly using exponential weighting. Apart from narrower lines this acquisition scheme also reduces artifacts elsewhere in the spectrum. The conventionally sampled spectrum is shown in blue, while the non-linear sampled spectrum is shown in red. The red spectrum was reconstructed using a non-linear Fourier transform and an artifact removal procedure described below.

Sampling schedule

The following time points were sampled in the indirect dimension (dwell time = 253.2 μ s):
td = 1 2 3 4 5 6 7 8 10 11 12 15 17 18 19 22 24 27 29 31 32 33 34 38 40 55 57 78 91 103 113 128

The data points were chosen randomly between 1 and 128 using an exponential weighting.

Processing of the non-uniform sampled 2D-HMQC spectrum

The direct dimension of the 2D-HMQC spectrum was transformed using a squared sine bell window function, zero filling up to 2048 data points and a standard fast Fourier transform. Standard 1D peak picking for the direct dimension was performed on the first 1D slice of a magnitude spectrum. The indirect dimension was reconstructed in several steps based on an algorithm described by Kazimierczuk et al. [*J Magn Reson* **2008**, 192, 123–130] including an analytical Fourier transform:

$$spc(\omega) = \frac{1}{\sqrt{2\pi}} \int_0^{\infty} FID(t) e^{i2\pi\omega t} dt$$

A non-linear Fourier transform leads to artifacts where the artifacts depend on signal intensity, frequency and sampling schedule. The reconstruction of the 2D spectrum therefore needs an artifact removal procedure which need several steps. The steps were as follows:

- The 2D spectrum was reconstructed using the analytical Fourier transform
- For the columns picked in the 1D spectrum plus three columns to the left and right the artifact removal procedure was performed. Picking 3 points around the signals was sufficient to include the entire line in the direct dimension.
- In each column picked in the 1D spectrum, the frequencies in the indirect dimension was determined by correlating pure complex sinusoids with the experimental FID.
- The data was then fitted to exponential decaying sinusoids.
- To get a better fit, a polynomial of order 8 was then fitted to the pure exponential functions to obtain a start parameter set for the next fitting procedure.
- With the start parameter set the amplitudes in each data point of a complex oscillating sinusoid were fitted to the experimental FID

$$FID(t_k) = A(t_k) e^{-i\omega t}, \quad A(t_k) = \sum_{l=0}^8 a_l t_k^l$$

- Using the fitted amplitudes and frequencies the spectrum was simulated for the entire spectral width and only 2.5 times the line width that was determined in the exponential model. The latter spectrum was then subtracted from the former. This way a spectrum containing only the sampling artifacts was obtained.
- Finally the artifact spectrum was subtracted from the experimental spectrum.

Radical signals in the hyperpolarized 2D-HMQC spectrum

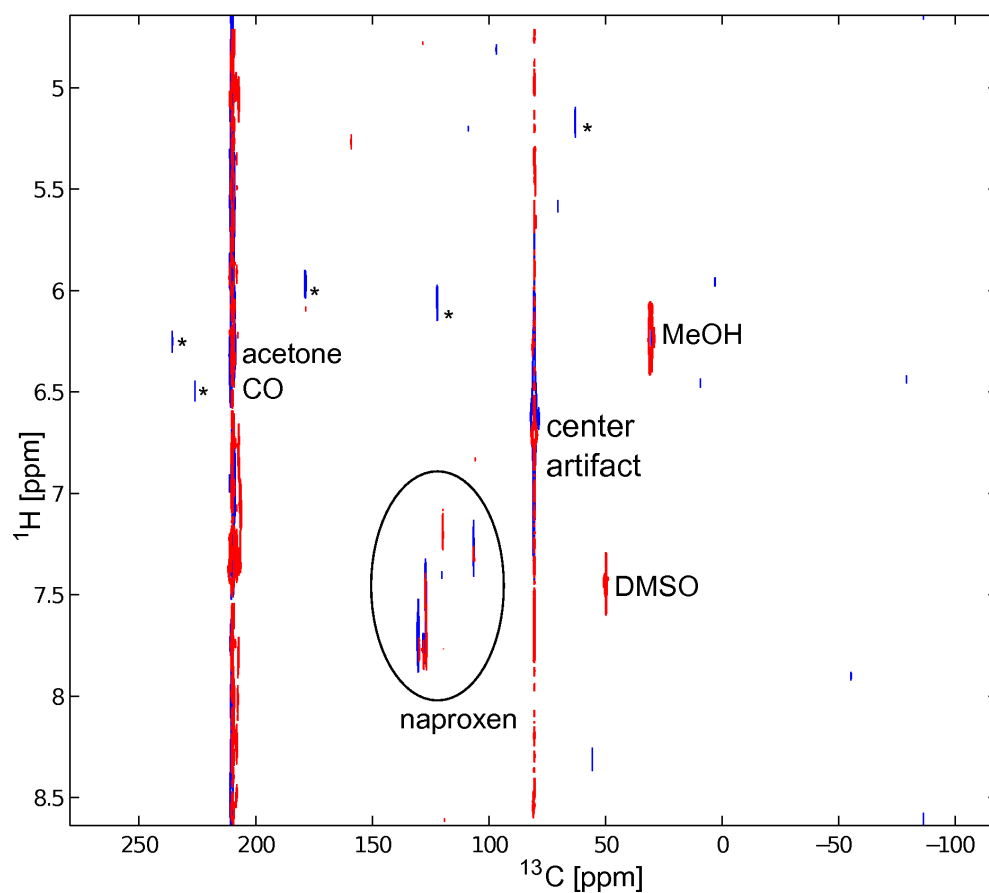


Figure S4. Full 2D spectrum of naproxen. Apart from the expected signals and those of DMSO and methanol. Artifacts of unknown origin are labelled with *.

Co-polarisation induced enhancement factors

The enhancement factor for several ^{13}C signals in naproxen and thiamine for DNP arising from the co-polarization agent:

Thiamine

Nucleus	Co-polarization vs no co-polarization agent present (both DNP)	Co-polarization agent (DNP) vs thermal spectrum (512 scans)
C_4	2.5	440
C_5	2.5	530
$\text{C}_{\text{P}2}$	2.2	370
$\text{C}_{\text{P}4}$	2.7	510
$\text{C}_{\text{P}5}$	2.8	420
$\text{C}_{\text{E}1}$	13.9	80
$\text{C}_{\text{Me}1}$	8.2	50
$\text{C}_{\text{Me}2}$	9.1	70

Naproxen

Nucleus	Co-polarization vs no co-polarization agent present (both DNP)	Co-polarization agent (DNP) vs thermal spectrum (512 scans)
C_2	2.5	45
C_4	1.7	90
C_5	3.8	75
C_7	3.9	85
C_9	1.8	50
C_{10}	3.8	60

Enhancements were calculated from integrated peak intensities using reference ^{13}C spectra with typically 1300 scans (ns). The relative number of transients was taken into account by multiplying the intensity ration with $\sqrt{\text{ns}}$.

Hyperpolarized 2D-HMQC spectrum of aspirin

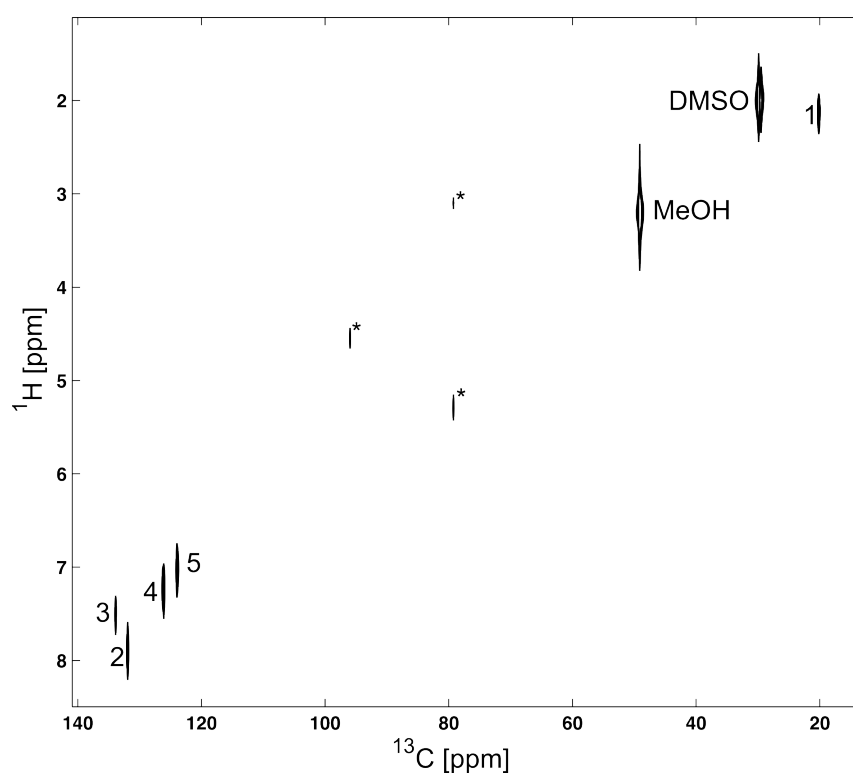


Figure S4. Full 2D spectrum of hyperpolarized aspirin with artifact signals (*). Apart from the expected signals and those of DMSO and methanol, additional signals (*) are observed which arise from the radical, impurities in the radical or from oxidization products of the same and are observed when the co-polarization agent is present.

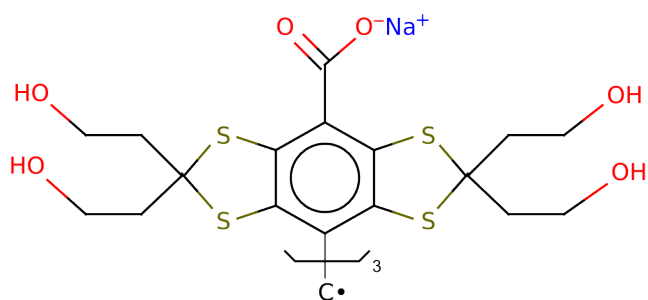


Figure S5. Structure of the Ox63 radical. Sytematic name: (tris{8-carboxyl- 2,2,6,6-tetra[2-(1-hydroxyethyl)]-benzo(1,2-d:4,5-dS)bis(1,3)dithiole-4-yl}methyl sodium salt).